# Photocatalytic Activity and UV-Protection of TiO$_2$ Nanocoatings on Poly(lactic acid) Fibres Deposited by Pulsed Magnetron Sputtering

J. O. Carneiro[1, *], V. Teixeira[1], J. H. O. Nascimento[1, 2], J. Neves[2], and P. B. Tavares[3]

[1] *Physics Department, University of Minho, Azurém Campus, 4800-058 Guimarães, Portugal*
[2] *Textile Engineering Department, University of Minho, Azurém Campus, 4800-058 Guimarães, Portugal*
[3] *Chemistry Department, University of Trás-os-Montes e Alto Douro, 5001-911 Vila Real, Portugal*

The application of nanocoatings in the textile finishing is increasingly being explored because they open a whole new vista of value-addition possibilities in the textile sector. In the present work, low temperature pulsed DC magnetron sputtering method was used to create functional TiO$_2$ nanocoatings on poly(lactic acid) textile fibres surfaces. In this study, the principal objectives in the application of TiO$_2$ nanocoatings to textile materials are to impart UV protection functions and self-cleaning properties to the textile substrates. The TiO$_2$ films were characterized by X-ray diffraction, scanning electron microscopy, atomic force microscopy, transmission electron microscopy, UV-visible spectroscopy and contact angle analysis. The Photocatalytic activity of the films was tested by measuring the photodegradation rates of rhodamine-B dye aqueous solution under UV light irradiation. The ultraviolet protection function was tested according to the Australian/New Zealand standards. It was observed that the TiO$_2$ nanocoatings on poly(lactic acid) fibres showed an excellent ultraviolet protection ($>$40) function and the photocatalytic efficiency was maintained even after a strong washing treatment.

**Keywords:** Titanium Dioxide, Nanocoatings, Textile Fibres, UV-Protection, Self-Cleaning.

**RESEARCH ARTICLE**

## 1. INTRODUCTION

The using of new techniques applied to the development of new materials, devices or systems in nanometrics scale is increasing in the recent years. Those new materials are receiving higher attention because due of their potentials applications in medicine, biology, microelectronics, photocatalysis, magnetic devices, powder metallurgy, renewable energies, and textile. Textile industries are using a new technology nanocoating, which is the application of a thin film of a material polymeric or not in a textile material. Researchers are inspired to mimic nature in order to create clothing materials with higher levels of functions and smartness. Textiles have mechanical, aesthetic, and material advantages that make them ubiquitous in both society and industry. Applied nanocoatings in textiles, clothing and textile for footwear have the objective to develop materials with properties antimicrobial, UV protection, water repellence, soil resistance, anti-static, anti-infrared, flame-retardant properties, colour fastness and strength of textile materials.

Poly(lactic acid) (PLA) is a biodegradable polymer which consists of linear aliphatic thermoplastic polyester derived from 100% of renewable sources such as corn. However, its most initial uses were limited to biomedical applications such as sutures and drug delivery systems due to availability and cost of manufacture. Nowadays, PLA is used broadly in textile applications due to the fact that PLA fibre is derived from annually renewable crops, it is biodegradable and its life cycle potentially reduces the Earth's carbon dioxide level.

Nanocrystalline titanium dioxide is widely used in different industrial areas[1] because of its unique properties such as photocatalytic, dermatological, antibacterial, deodorization, antifogging, anti-algal oil proofing, and decomposition of various environmental pollutants in both gases and liquid phases.[2–3]

TiO$_2$ nanocoatings can be synthesized by a number of different deposition techniques. On the particular case of textile materials substrates, many studies has been performed related with the preparation of TiO$_2$ nanocoatings by a variety of deposition techniques such as plasma enhanced chemical vapour deposition,[4] sol–gel method on cotton, wool and polyethylene terephthalate,[5–11] liquid

---

phase deposition on carbon fibres,[12] DC magnetron sputtering on polyester nonwoven[13] and RF sputtering on polypropylene fibres.[14] However, low temperature synthesis processes are best suitable in the case of temperature-sensitive substrate materials. Among these deposition methods, pulsed DC magnetron sputtering (PMS) has come to get a particular interest in the sputtering field, since it can be used to prepare, at low substrate temperature, high quality thin films (high density, strong adhesion, high hardness, better transparency and good uniformity over large areas), because it reduces or eliminate arcs during the deposition process.[15–17]

The application of nano-particles to textile materials has been the object of several studies intended to produce finished fabrics with different performances. For example, the antibacterial function of TiO$_2$ photocatalyst is markedly enhanced with the aid of either silver or copper,[18–19] which is harmless to the human body. In addition, titanium dioxide is non-toxic and chemically stable under exposure to high temperatures, and capable to impart photocatalytic oxidation and self-cleaning properties.

This paper discusses the steps involved in the preparation of TiO$_2$ nanocoatings deposited on PLA substrates by means of PMS. Because wash fastness is a particular requirement for textile (due to the fact that it is strongly related with the thin film adhesion to the fibres), some TiO$_2$ coated samples were subjected to washing treatments (according a standardized test) in order to evaluate this effect on the photocatalytic activity, self-cleaning properties and UV-protection function.

### 1.1. TiO$_2$ Photocatalytic Activity

Photocatalysis originates from the oxidation and reduction potential of titania induced by UV radiation. When UV light with a higher energy than the titania band-gap (3.0–3.2 eV) is illuminated on its surface, inter band transition is induced resulting in the generation of electron–hole ($e^-/h^+$) pairs. Such excited electrons or holes can diffuse to the surface and generate types of radicals or ions that in turn will decompose organic compounds adsorbed on the titania surface. This means that titania can be used as a photocatalyst to promote oxidation and reduction reactions of toxic organic compounds to non-toxic inorganic compounds, such as carbon, water, ammonium or nitrates and chloride ions. The TiO$_2$ photocatalytic mechanism is well is well described elsewhere.[20]

### 1.2. Self-Cleaning Properties

The traditional surface cleaning of materials, sometimes causes considerable troubles, because it needs the use of chemical detergents, high consumption of energy, and consequently high costs. In order to obtain self-cleaning

material surfaces, there are two principal ways: the development of the so-called hydrophilic (or hydrophobic) surfaces. The surface wettability is generally evaluated by the water contact angle (CA) which is defined as the angle between the solid surface and the tangent line of the liquid phase at the interface of the solid–liquid–gas phases. Initially a TiO$_2$ thin film exhibits a CA of several tens of degrees depending on the surface conditions namely its surface roughness. When this surface is exposed to UV light, water starts to exhibit a decreasing in the CA (reaching almost 0°), that is, it tends to spread out flat. At this phase, the surface becomes completely non-water-repellent and is called 'super-hydrophilic.' On the opposite side, a CA of 180° corresponds to a complete non-wetting, the so called 'super-hydrophobic' surfaces. According some authors, when a TiO$_2$ surface is irradiated with UV light a completely clean surface can be obtained by a photocatalytic reaction and by some structural changes (being responsible for a highly hydrophilic state) on TiO$_2$ surfaces.[21]

### 1.3. Ultraviolet Protection

Throughout the world, there is an increasing frequency of skin cancer.[22] For example, more than one million new cases of skin cancer are diagnosed in the United States;[23] furthermore, more than half of all new cancers in the US are skin cancers. According the American Cancer Society, about 80% of these new skin cancer cases are basal cell cancer, 16% are squamous cell, and 4% are melanoma cancer (the incidence of melanoma more than tripled among American Caucasians between 1980 and 2004).

Even though that there are many factors that induce the development of skin cancers, the principal environmental factor is the UV exposure of an individual. Actually, in the last years many studies have concluded that an excessive exposure to UV light and an insufficient protection by clothing, contributes to the skin cancer epidemic, as well as creating health problems in patients suffering from photosensitive diseases. While the best technique for reducing UV exposure is to avoid the sun, this solution is unacceptable in the present global society. In this sense, sun-protection has been recently fixed on sun-protective clothing, designed to block UV-A and UV-B radiation. Sun-protective clothing gives consumers an effective path to prevent skin diseases. However, the assumed protective benefits in the utilization of regular clothing have been recently questioned because some studies[24] have shown that many textiles provide only limited UV protection.

## 2. EXPERIMENTAL DETAILS

### 2.1. Material Preparation

The TiO$_2$ nanocoatings were deposited on 100% commercial PLA fibres of (10 cm × 10 cm), with a mass of 2 g/cm$^2$

and fibre fineness of 19.667 Tex. Before coating deposition, the substrates were first washed with distilled water and non-ionic detergent at 40 °C for 30 min.

## 2.2. Synthesis of $TiO_2$ Nanocoatings by Pulsed DC Magnetron Sputtering

During DC reactive magnetron sputtering deposition of an oxide from a metal target in a mixture of argon and oxygen environment, the target is oxidized and an insulating layer is formed on its surface. This insulating layer is positive charged by the ions that are in the plasma and came together with the surface target. However, when the insulating layer cannot withstand any longer the electric field strength, an electrical breakdown occurs in the layer in the form of an electrical arc.[25–26] These arc events lead to the ejection of droplets of material from the target surface that can cause defects and lack of stoichiometry in the growing film, which consequently deteriorates the optical and electrical properties.

Using a pulsed DC power supply the occurrence of arc events can be suppressed or significantly reduced. The voltage build on the insulating layer may be restricted by applying a short positive pulse to the target. During the positive part of the pulsed period electrons are collected at the target surface, and due to the fact that they have lower mass compared to the ions, they have also much higher mobility. In this sense, the discharge current (positive part) will be much higher than the charging current (negative part) and thus it will prevent the occurrence of arcs, resulting in a stable, controllable and repeatable process.[25–26] There are two modes of pulsed DC operation: unipolar pulsed sputtering, where the target voltage is pulsed between the normal operating voltage and ground; and the bipolar pulsed sputtering, where the target voltage is reversed and becomes positive during the pulse-off period. For a particular reverse time ($t_r$), a part of each pulse has a positive reverse voltage, which is called the reverse phase and accounts for 10–50% of each pulse, and the remaining (90–50%) is called as duty cycle, where the sputtering erosion of the target happens.

Due to the higher mobility of electrons in the plasma, it is only necessary to reverse the target voltage between 10% and 20% of the negative operating voltage to fully dissipate the charged regions and prevent arcing. This mode (in which the target voltage is not fully reversed), schematized in Figure 1, is referred as asymmetric bipolar pulsed DC.

As can be observed (Fig. 1) there are two adjustable parameters: frequency and reverse time. The frequency is related to the wave that modulates the voltage; while the reverse time is the time when no power is transferred to the plasma, and the voltage is reversed (10%–40% of the voltage becomes positive). These two parameters are related to the duty cycle as referred previously. The duty cycle
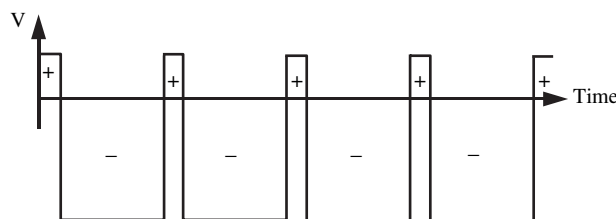


**Fig. 1.** Schematic representation of the target voltage (V) waveform for a pulsed DC power supply operating in asymmetric bipolar pulse mode.

is referred to the sputter time, and it is the ratio between the time when the voltage is negative and the period of the pulse. The reverse phase, $\tau_r$ is given by the following equation:

$$\tau_r = \frac{t_r}{T} \times 100 \qquad (1)$$

where $t_r$ is the reverse time and $T$ is the period of the pulse. In the present study an asymmetric bipolar pulsed DC power supply system (Advanced Energy Pinnacle Plus 5 K DC Pulsed) is used at room temperature, where the reverse phase is 40%. The target was titanium with a purity of 99.9% and a total surface area (TA) of 7854 $mm^2$. The distance between target and substrate was 60 mm. Before starting the deposition process, the sputtering chamber was pumped down to a pressure of $10^{-5}$ mbar. After the chamber has been evacuated to a base pressure lower than $1 \times 10^{-3}$ mbar, a 99.9% pure argon sputtering gas was introduced into the chamber at a constant current of 0.45 A. The typical deposition parameters used to produce the $TiO_2$ nanocoatings are listed in Table I.

## 2.3. Characterization of Nano-$TiO_2$ Coated Fabrics

The crystal structure of the films was determined using X-ray diffraction (XRD) with a $CuK_\alpha$ radiation source using a Philips PW 1710 BASED diffractometer. The obtained results were used to determine the crystallographic structure and the phase quantities, using the Rietveld structural refinement technique using the PowderCell 2.4 software. The average crystallite grain size of $TiO_2$ coatings was calculated by the Scherrer's equation[27] after the full width of peak at half of maximum intensity (FWHM) determination.

The surface morphology and microstructure of the films was observed by AFM using a NANOSCOPE III Digital instrument, by SEM in a LEICA Cambridge S360 instrument, and by TEM in a LEICA LEO 906E intrument. The

**Table I.** Deposition parameters to prepare $TiO_2$ nanocoatings by pulsed DC magnetron sputtering.

| Pressure (mbar) | Flow rate $O_2$:Ar (sscm) | Reverse time ($\mu$s) | Frequency (kHz) | Current (A) | Deposition time (min) | Deposition rate (nm/min) |
|---|---|---|---|---|---|---|
| $4.2 \times 10^{-3}$ | 2.5:10 | 2.0 | 200 | 0.45 | 30 | 2.53 |

optical properties of the TiO$_2$ nanocoatings were evaluated on a glass substrate by UV-visible spectrophotometer Shimadzu UV 3101 PC, in the spectral wavelength range from 280 nm to 1100 nm.

The photocatalytic activity of TiO$_2$ nanocoatings was evaluated by measuring the transparency of a strong red fluorescent dye, rhodamine-B (C$_2$H$_{31}$ClN$_2$O$_3$) aqueous solution as a function of irradiation time. The initial concentration of RhB solution used in this study was 0.5 mg/L. The photodegradation efficiency of the RhB aqueous solution was monitored by measuring its optical transmittance as a function of irradiation time, at a wavelength of 553 nm (which corresponds to the S$_0 \rightarrow$ S$_1$ excitation of the RhB molecules) using the UV-visible spectrophotometer. An increase in the transmittance of the solution should indicate the decomposition of the RhB dye by TiO$_2$ photocatalysis.

In order to evaluate the hydrophobic-hydrophilic properties of the TiO$_2$ nanocoatings, dynamic contact angle measurements (contact angle between a liquid and a solid) were carried out by using a Goniometer System OCA-15 (software SCA 20). The drop image (water drop size of 10 $\mu$L) is stored via a video camera using a PC-based control acquisition and data processing.

Washings were carried out (according to the Standard ISO 105 C06 – N° A1S) in order to evaluate the adhesion of TiO$_2$ nanocoatings on the surface of PLA textile fibres. Under the occurrence an eventual scenario, characterized by a significant decrease in UV-blocking properties and photocatalytic efficiency, then the TiO$_2$ adhesion on the surface of textile fibres should be weak. In the present work, it was used a Linitest Plus apparatus (Atlas, Gelnhausen, Germany) under a rotation motion of 40 rpm and a temperature laundering bath of 40 °C for 30 minutes. The laundering solution was prepared by dissolving 4 g/L of a commercial detergent in distilled water. The laundering cycle was repeated 10 times. The samples drying are made at room temperature.

A relatively new rating designation for sun-protective textiles and clothing is given by the ultraviolet protection factor (UPF) values. The UPF values were calculated according to the Australian/New Zealand Standard AS/NZS 4399:1996. Measurements were performed in a UV-visible spectrophotometer system SDL, model M284, from 295 nm at an interval of 1 nm. The percentage blockings of UV-A (315 nm–400 nm) and UV-B (295 nm–315 nm) were calculated from the transmittance data. The UV protection factor (UPF) was calculated using the following equation:[28]

$$UPF = \frac{\sum_{\lambda_1}^{\lambda_2} E_\lambda \times S_\lambda \times \Delta\lambda}{\sum_{\lambda_1}^{\lambda_2} E_\lambda \times S_\lambda \times T_\lambda \times \Delta\lambda} \qquad (2)$$

where $E_\lambda$ is the relative erythemal spectral effectiveness, $S_\lambda$ is the solar spectral irradiance (in W/m$^2$·nm$^{-1}$), and $T_\lambda$ is the spectral transmission of the specimen, and $\Delta\lambda$ is the measured wavelength interval (nm).
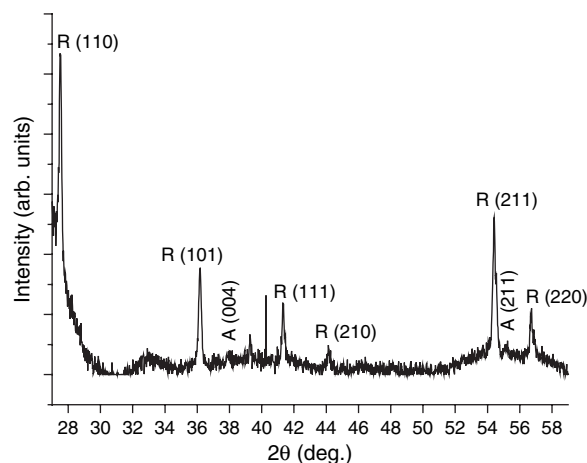


**Fig. 2.** XRD pattern of the TiO$_2$ nanocoatings produced via PMS.

## 3. RESULTS AND DISCUSSION

The results obtained and their discussions are as follows.

### 3.1. TiO$_2$ Crystallographic Structure and Phase Quantities

The Figure 2 shows the XRD (X-ray diffraction) spectrum of the TiO$_2$ nanocoatings. The identification of the film crystalline phases was carried out by the Rietveld structural refinement method using the Powder Cell 2.4 software.

As can be observed, the polycrystalline rutile structure is well defined by the (110), (101), (111), (211) and (220) diffraction peaks and also traces of anatase structure confirmed by the (004) and (211) diffraction peaks. The mean crystalline grain sizes of the films are listed in Table II, and were calculated from the full with at half-maximum of the diffraction peak according to the Scherrer's equation.

### 3.2. Surface Morphology

The Figure 3 shows an AFM image of the TiO$_2$ thin films. The surface reveals a certain degree of roughness and exhibit the typical columnar growth with some structural densification.

The following figures show the SEM micrographs of TiO$_2$ coated PLA textile fibres. The Figure 4 shows a SEM micrograph of the surface of a TiO$_2$ coated PLA textile fibre under higher magnification, which show evidence of the film thickness ($\sim$75.8 nm).

**Table II.** TiO$_2$ mean crystalline grain sizes and its phase quantity percentage.

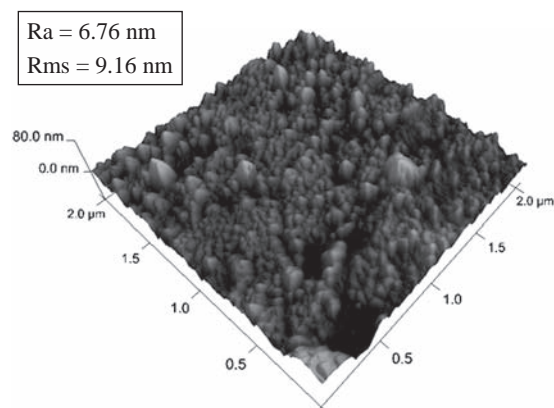| Sample | Anatase (%) | Grain size (nm) | Rutile (%) | Grain size (nm) |
|---|---|---|---|---|
| TiO$_2$/PLA | 24.5 | 14.34 | 75.5 | 14.88 |

**Fig. 3.** AFM images of TiO$_2$ nanocoatings produced via PMS.

The Figures 5(a, b) shows the SEM micrographs (under low magnification) of TiO$_2$ coated surface of PLA textile fibres, respectively without and with washing treatments.

The as-deposited TiO$_2$ thin films (Fig. 5(a)) on PLA substrate had covered the entire surface of the PLA textile fibres, revealing good adhesion. However, for the samples that had been subjected to washing treatments (Fig. 5(b)), it can be observed the presence of some cracks and also some large uncoated regions. This situation evidences that washing treatments lead to some adhesion losses.

Compared with SEM, TEM has better spatial resolution. The Figure 6 represents a TEM micrograph (under higher magnification) which shows the size, shape and arrangement of the crystalline TiO$_2$ nanocoatings deposited by PMS. The scale bar of the micrograph corresponds to 100 nm.

As can be observed, the TiO$_2$ nanocoatings present a columnar arrangement, with spherical crystalline nanograins, where its size varies between 10–12 nm and 15–42 nm, which agrees with the XRD results.
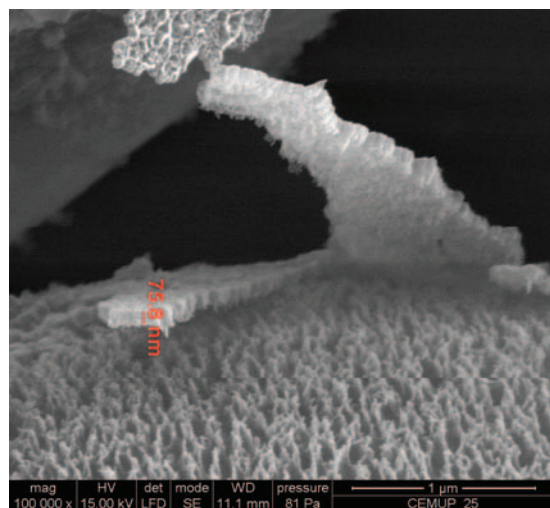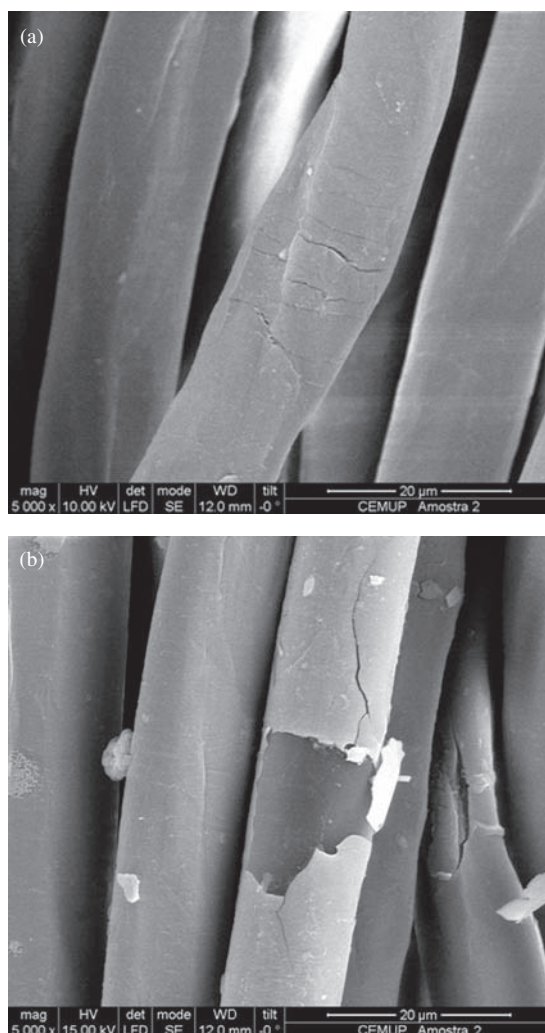


**Fig. 5.** SEM micrographs of TiO$_2$ coated surface of PLA textile fibres: (a)—without washing treatments; (b)—with washing treatments.
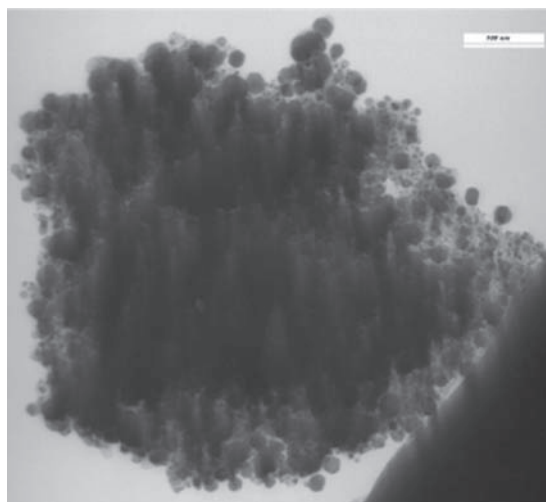


**Fig. 4.** SEM micrograph of TiO$_2$ coated PLA textile fibres.



**Fig. 6.** TEM micrograph of TiO$_2$ nanocoatings deposited by PMS.

RESEARCH ARTICLE

## 3.3. Evaluation of the TiO$_2$ Photocatalytic Activity

The photocatalytic behaviour of the titania coatings was assessed by combined ultraviolet irradiation and transmittance measurements. Analysis of the transmittance data allows us to obtain the decrease in RhB concentration ($C$) as a function of UV irradiation time. Figure 7 compares the variation in RhB concentration promoted by coated TiO$_2$ samples, respectively before and after washing treatments. It is obvious that $C_0$ represents the initial concentration of RhB (i.e., before UV irradiation). In addition, it should be noted that, under similar UV irradiation conditions, the absence of a photocatalyst material did not affect the dye's concentration.

It is observed that TiO$_2$ samples that had been subjected to washing treatments have slightly lower photo-decomposition ability than that of the as-deposited TiO$_2$ samples (without washing). Possible explanations could be based on the fact that TiO$_2$ samples which had been subjected to washing treatments, exhibit some cracks and uncoated regions; therefore they have a lower active surface area to promote the photocatalysis process. Nevertheless, in both cases the photocatalysis process occurred efficiently. This indicates that nanosized particles should enhance photocatalytic activity. In fact, as the grain size is decreased the surface-to-volume ratio is increased and the photo-generated electrons and holes could undergo a short pathway to migrate to the surface. Thus, the ($e^-/h^+$) volume recombination rate should decrease, giving rise to an improvement in photocatalytic activity.

## 3.4. Photo-Induced Hydrophilicity

As previously referred, a surface wettability is generally evaluated by the water contact angle. Figure 8 shows the changes in CA that have been obtained under light irradiation.

It can be observed that before light irradiation the TiO$_2$ coated surface is highly hydrophobic with a CA of about
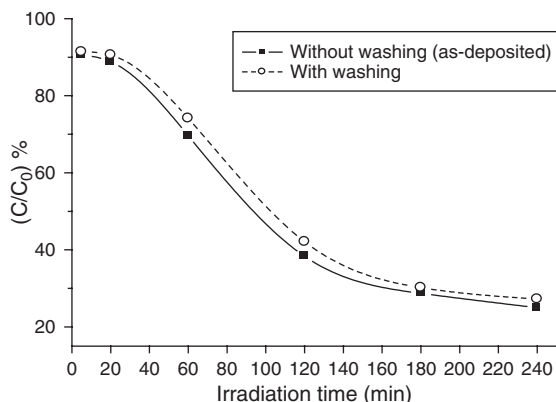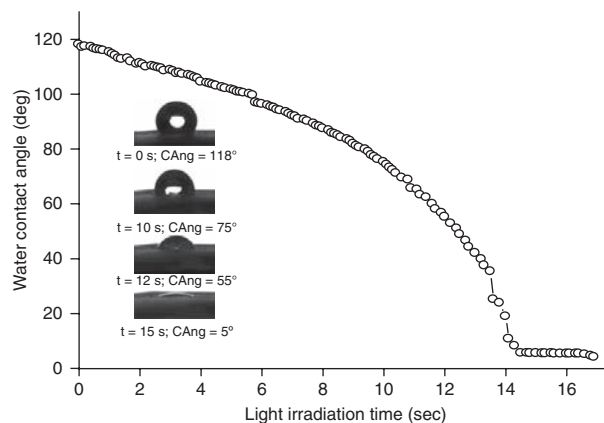


**Fig. 8.** Changes in the water contact angle of TiO$_2$ coated PLA textile fibres.

118°. For a non-flat surface, surface roughness affects the wettability. In fact, we have obtained TiO$_2$ rough surfaces, as can be seen in Figure 3. Thus, the hydrophobic TiO$_2$ surface requires surface roughness where air can intrude between the water droplet and the TiO$_2$ surface. Meanwhile, after light exposition we can observe that contact angles decreased to almost 0°, that is, the TiO$_2$ surface becomes highly hydrophilic, suggesting the presence of a structural surface changes due to the formation of new OH groups (at the titanium site) produced by light irradiation.[21] Because a water droplet is substantially larger than the hydrophilic domains, it instantaneously spreads completely on the surface, thereby resembling a two-dimensional capillary phenomenon.[21] These results show that TiO$_2$ thin films have a wide range of industrial applications. In fact, they have a very effective self-cleaning function because pollutants can be partially decomposed by the photocatalytic reaction, as well as washed by water due to the photo-induced hydrophilicity effect.

## 3.5. Ultraviolet Protection Factor (UPF)

The ability of a textile material to block UV light is given by the UPF factor. The UPF factor was calculated according to Australian/New Zealand Standard tests methods. According this standard, a UPF rating of (15–24) is classified as "Good Protection" whereas (UPF 25–39) and (UPF > 40) are classified, respectively as "Very Good Protection" and "Excellent Protection." For example, a textile material with a UPF of 30 only allows 1/30th of the UV radiation falling on the surface of the material to pass through it. That is, it blocks 29/30ths or ~97% of the UV radiation.

Figure 9 shows the UPF factors, respectively for the bare PLA samples (that is, without a TiO$_2$ film and without a washing treatment), TiO$_2$ coated PLA samples (i.e., without washing treatment) and TiO$_2$ coated PLA samples subjected to washing treatments.
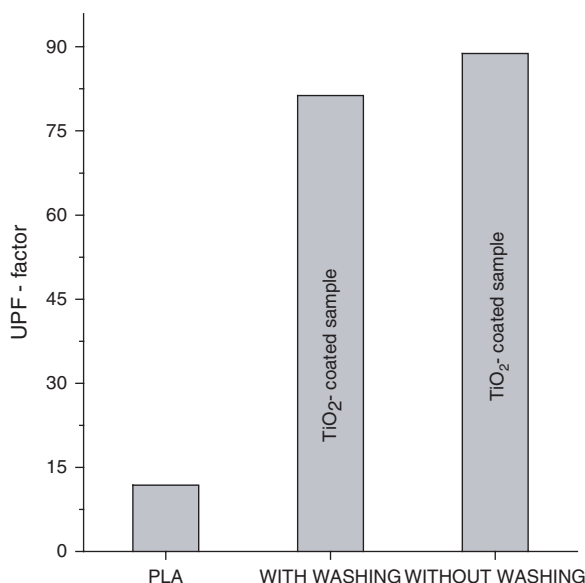


**Fig. 7.** Relative reduction in RhB concentration as a function of time, induced by TiO$_2$ films.

**Fig. 9.** UPF factors of TiO$_2$ coated PLA fabrics (treated and untreated), and bare PLA.

We can observe that both of nano-TiO$_2$ coated PLA samples showed a very efficient blocking of UV radiation and thus, they can be classified as "Excellent Protection." The UPF factor for the untreated TiO$_2$ coated PLA sample (i.e., without washing treatment) is calculated to be 88.8, while it is 81.3 for the TiO$_2$ coated PLA sample subjected to the washing treatment; that is, only a decrease of about 8% has been registered for the UPF factor. From this data, it can be construed that the washing treatment has not practically any effect in the efficiency of UV protection. This fact dictates that, nevertheless the washing treatment, the adhesion of the TiO$_2$ nanocoatings to the PLA fibres is still maintained. Meanwhile, the UPF factor for the bare PLA sample is calculated to be 11.8, and thus it can be classified as "Poor Protection." These findings enable us to affirm that TiO$_2$ nanocoatings play a strong and decisive role in the enhancement of the efficiency of UV protection.

## 4. CONCLUSIONS

Based on the results from the experimental study the following conclusions can be highlighted.

This work presents an important method to prepare TiO$_2$ nanocoatings and their application onto PLA textile fibres imparts self-cleaning and UV protection functions. TiO$_2$ nanocoatings were analysed via electron microscopy and X-ray diffraction. The mean crystalline grain sizes of TiO$_2$ particles is estimated to be 14.7 nm, using XRD data, which was confirmed by TEM.

It was also shown that the TiO$_2$ nanocoatings deposited on PLA textile fibres exhibited excellent self-cleaning and UV protection functions as well as photocatalytic activity, nevertheless some washing treatments to which they had

been subjected. In addition it was also shown that surface roughness affected the TiO$_2$ surface wettability (that is, affects the photo-induced hydrophobic/hydrophilic surface conversion).

Unquestionably, we believe that techniques applied to the development of new materials in nanometrics scale (nanotechnology), holds a strong promising future for textile industry and for the consumers.

## References and Notes

1. K. Qi, W. A. Daoud, J. H. Xin, C. L. Mak, W. Tang, and W. P. Cheung, *J. Mater. Chem.* 16, 4567 (**2006**).
2. D. Chatterjee and S. Dasgupta, *J. Photochem. Photobiol. C: Photochem. Review.* 6, 186 (**2005**).
3. Z. Liuxue, L. Peng, and S. Zhixing, *Mater. Chem. Phys.* 98, 111 (**2006**).
4. H. Szynabiwski, A. Sobczyk, M. Gazicki-Lipman, W. Jakubowski, and L. Klimek, *Surf. Coat. Technol.* 200, 1036 (**2005**).
5. Y. Dong, Z. Bai, L. Zhang, R. Liu, and T. Zhu, *J. App. Polymer. Sci.* 99, 286 (**2006**).
6. P. Xu, X. Liu, W. Wang, and S. Chen, *J. App. Polymer. Sci.* 102, 1478 (**2006**).
7. M. J. Uddin, F. Cesano, F. Bonino, S. Bordiga, G. Spoto, D. Scarano, and A. Zecchina, *J. Photochem. Photobiol. A: Chem.* 189, 286 (**2007**).
8. B. Fei, Z. Deng, J. H. Xin, Y. Zhang, and G. Pang. *Nanotechnology* 17, 1927 (**2000**).
9. W. S. Tung and W. Daoud, *Acta Biomaterialia* 5, 50 (**2009**).
10. T. Yuranova, D. Laub, and J. Kiwi, *Catal. Today* 122, 109 (**2007**).
11. K. Qi, J. H. Xin, W. A. Daoud, and C. L. Mak, *Int. J. App. Ceramic Technol.* 4, 554 (**2007**).
12. B. Herbig and P. Löbmann, *J. Photochem. Photobiol. A: Chem.* 163, 359 (**2004**).
13. Y. Xu, N. Wu, Q. Wei, and X. Pi, *J. Coat. Technol. Res.* http://dx.doi.org/10.1007/s11998-008-9149-x (**2008**).
14. Q. Wei, L. Yu, R. R. Mather, and X. Wang, *J. Mater. Sci.* 42, 8001 (**2007**).
15. J. Sellers, *Surf. Coat. Technol.* 98, 1245 (**1998**).
16. P. J. Kelly, C. F. Beevers, P. S. Henderson, R. D. Arnell, J. W. Bradley, and H. Bäcker, *Surf. Coat. Technol.* 174–175, 795 (**2003**).
17. J. T. Chang, C. W. Su, and J. L. He, *Surf. Coat. Technol.* 200, 3027 (**2006**).
18. H. J. Lee, S. Y. Yeo, and S. H. Jeong, *J. Mater. Sci.* 38, 2199 (**2003**).
19. K. Sunada, T. Watanabe, and K. Hashimoto, *Environ. Sci. Technol.* 37, 4785 (**2003**).
20. J. O. Carneiro, V. Teixeira, A. Portinha, A. Magalhães, P. Coutinho, C. J. Tavares, and R. Newton, *Mater. Sci. Eng., B* 138, 144 (**2007**).
21. K. Hashimoto, H. Irie, and A. Fujishima, *Jpn. J. Appl. Phys.* 44, 8269 (**2005**).
22. K. Hoffmann, J. Laperre, A. Avermaete, P. Altmeyer, and T. Gambichler, *Arch Dermatol.* 137, 1089 (**2001**).

**RESEARCH ARTICLE**

**23.** R. Edlich, M. Cox, D. Becker, J. Horowitz, L. Nichter, L. D. Britt, T. J. Edlich, and W. B. Long, *Journal of Long-Term Effects of Medical Implants.* 14, 95 **(2004)**.

**24.** P. Gies, C. Roy, S. Toomey, and D. Tomlinson, *J. Epidemiol.* 9, S115 **(1999)**.

**25.** P. J. Kelly and R. D. Arnell, *Vacuum* 56, 159 **(2000)**.

**26.** L. B. Jonsson, T. Nyberg, I. Katardjiev, and S. Berg, *Thin Solid Films* 365, 43 **(2000)**.

**27.** R. H. Jenkins and R. L. Snyder, Introduction to X-ray Powder Diffractometry, John Willey and Sons, New York **(1996)**.

**28.** S. Kathirvelu, L. D'Souza, B. Dhurai, *Mater. Sci.* 15, 1392 **(2009)**.

**RESEARCH ARTICLE**